

Special
Collection

Industrially Relevant Conditions in Lab-Scale Analysis for Alkaline Water Electrolysis

Niklas Thissen,^{*[a]} Julia Hoffmann,^[b, c] Sebastian Tigges,^[d] Dominik A. M. Vogel,^[a] Jil J. Thoede,^[a] Stefanie Khan,^[a] Nicolai Schmitt,^[b] Saskia Heumann,^[d] Bastian J. M. Etzold,^[b, c] and Anna K. Mechler^{*[a]}

Alkaline water electrolysis remains one of the most promising technologies for the large-scale production of green hydrogen. However, further increases in efficiency remain elusive, as new electrode materials that are highly efficient in the laboratory cannot maintain their performance under industrial conditions. Within this work, we present a beaker cell setup, in which the industrial relevance of research materials can already be

investigated in the laboratory by applying industrial conditions. Thus, the setup allows for testing at 80 °C in 30 wt.% KOH for more than 300 hours. Electrodes are contacted with an in-house designed Ni tuck-in holder and two types of reference electrodes are recommended. In addition, a protocol to unify catalyst research is introduced.

Introduction

Alkaline water electrolysis (AWE) is one of the most fundamental and promising processes for producing green hydrogen, a versatile energy carrier that can substitute fossil fuels and decrease carbon emissions.^[1,2] Among other water electrolysis technologies, AWE's key advantage lies in providing a stable performance without the use of scarce noble metals.^[3,4] However, the major bottleneck preventing this technology to be widely spread in energy systems is its relatively poor energy efficiency even at low current densities. This is not only caused by the use of thick diaphragms but also by a lack of efficient electrocatalysts, especially to improve the sluggish oxygen evolution reaction (OER).^[5] Therefore, in the past decades,

countless noble metal-free catalyst materials have been developed and investigated.^[6] In fact, some materials even outperformed state-of-the-art catalysts in terms of OER activity under laboratory conditions.^[7–10] However, hardly any of these materials could be applied in industry, because catalysts that are highly active on a laboratory scale do not automatically maintain their performance under industrial conditions.^[11,12]

To achieve successful innovation transfer, it is necessary to conduct laboratory experiments that closely resemble industrial conditions in terms of electrode design and experimental conditions (see Figure 1). Industrial applications typically use Ni meshes as the support material for their electrodes, since they provide a large surface area. This not only increases the number of available active sites, but also facilitates the removal of bubbles.^[13] Furthermore, these supports can be welded to the current collectors, which is especially important on the anode side.^[14] To improve kinetics and simplify heat management, commercial electrolyzers are operated at elevated temperatures of 80–90 °C.^[15] At this temperature, electrolyte concentrations of ~30 wt.% KOH (~7 M KOH) are used, providing high conductivity in order to minimize the electrolyte resistance.^[4] In the past, AWE was operated at relatively low current densities of 200–400 mA cm⁻².^[16,17] In fact, nowadays, electrode manufacturers specify a maximum current density of up to 1,200 mA cm⁻². As a lifetime, more than 5 years with negligible performance drift are guaranteed for some of the electrode packages.^[18]

At present, the only setup being able to fulfill most of the industrial criteria in the laboratory is the flow-cell setup (full single cell with continuous electrolyte flow). Herein, electrode type, temperature, KOH concentration, and current densities can reach industrial conditions. However, closely looking at the electrode of interest by introducing a reference electrode (RE) can hardly be realized. Furthermore, the buildup of this type of test stand is too complex and hence expensive to be widely available in research laboratories and too time-consuming for fast catalyst screening and optimization.^[14,19] Therefore, only a few materials have been tested under industrial conditions so

[a] N. Thissen, D. A. M. Vogel, J. J. Thoede, S. Khan, Prof. A. K. Mechler
Electrochemical Reaction Engineering (AVT.ERT)
RWTH Aachen University
Forckenbeckstraße 51, 52074 Aachen, Germany
E-mail: niklas.thissen@avt.rwth-aachen.de
anna.mechler@avt.rwth-aachen.de

[b] J. Hoffmann, N. Schmitt, Prof. B. J. M. Etzold
Ernst-Berl-Institute for Technical Chemistry and Macromolecular Science
Technische Universität Darmstadt
Alarich-Weiss-Straße 8, 64287 Darmstadt, Germany

[c] J. Hoffmann, Prof. B. J. M. Etzold
Power-To-X Technologies
Friedrich-Alexander-Universität Erlangen-Nürnberg
Dr. Mack Str. 81, 90762 Fürth, Germany

[d] Dr. S. Tigges, Dr. S. Heumann
Max Planck Institute for Chemical Energy Conversion
Stiftstraße 34–36, 45470 Mülheim an der Ruhr, Germany

Supporting information for this article is available on the WWW under <https://doi.org/10.1002/celec.202300432>

This publication is part of a Special Collection on Holistic Development of Electrochemical Processes for Industrial Systems

© 2023 The Authors. ChemElectroChem published by Wiley-VCH GmbH. This is an open access article under the terms of the Creative Commons Attribution License, which permits use, distribution and reproduction in any medium, provided the original work is properly cited.

Rotating Disc Electrode (RDE)	Setup	Electrochemical Flow-Cell	
		Laboratory	Industry
Glassy Carbon (GC)	Electrode Support	Ni Mesh (woven / expanded)	
0.001 – 0.05 mg cm ⁻²	Catalyst Loading	1 – 20 mg cm ⁻²	
0.1 - 1 M NaOH / KOH (~0.5 - 5 wt.%)	Electrolyte Concentration	1 - 7 M KOH (~5 - 30 wt.%)	7 M KOH (~30 wt.%)
20 - 80 °C (mostly room temperature)	Temperature	20 - 80 °C	80 - 90 °C
10 - 100 mA cm ⁻² (mostly 10 mA cm ⁻²)	Current Density	100 - 1,200 mA cm ⁻²	
Minutes to Hours	Experiment Duration	Days to Weeks	5 – 10 years

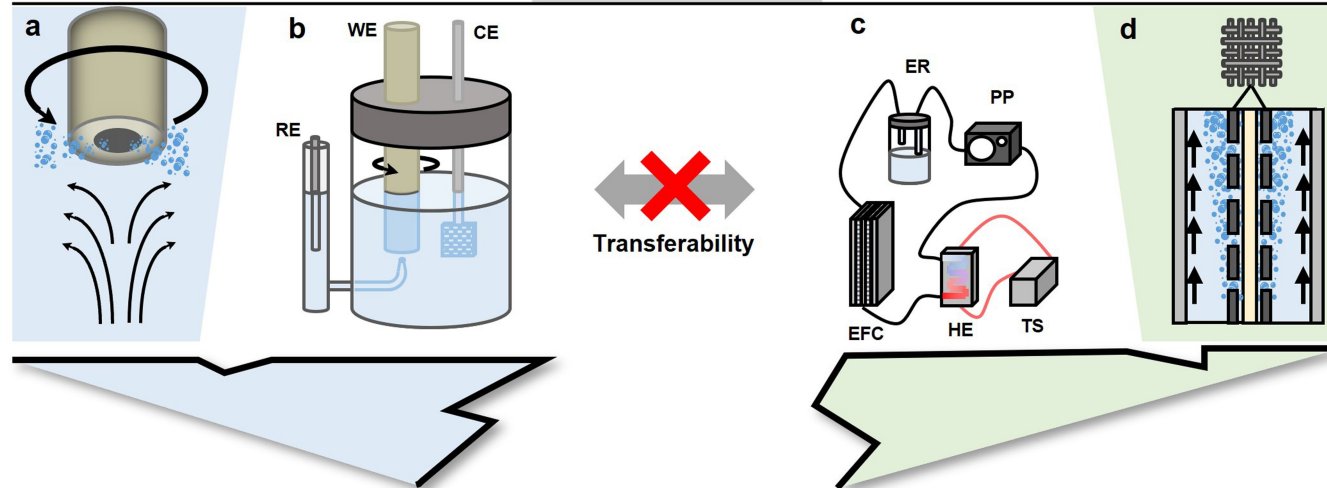


Figure 1. Local environment of an RDE working electrode in operation (a). Schematic representation of an RDE setup including working electrode (WE), counter electrode (CE), and reference electrode (RE) connected by a Luggin capillary (b). Schematic diagram of a simplified flow-cell setup including the electrochemical flow-cell (EFC), the electrolyte reservoir (ER), a peristaltic pump (PP), a heat exchanger (HE) & thermostat (TS) (c). Schematic design of a flow-cell for alkaline water electrolysis (bottom) and a metal mesh electrode (d). The table above summarizes the most important characteristic features of the RDE (left column) and the electrochemical flow-cell (EFC, right), subdivided into laboratory EFCs and industrial EFCs.

far.^[20–22] The remaining materials are tested with classical electrochemical laboratory setups such as the rotating disk electrode (RDE), which enables quick and accessible characterization of new materials, but reduces the industrial relevance of the results drastically.^[23–26]

For the RDE, a few micrograms of catalyst are immobilized on a glassy carbon support using a Nafion® binder. This procedure is prone to error and imprecise, and thus, the reproducibility of RDE experiments is questionable.^[27,28] The temperature and KOH concentrations of such experiments are typically set to 25 °C and 1 M KOH or NaOH due to material corrosion of the rotating electrode. In order to investigate the intrinsic performance of the catalysts, many researchers also purify their electrolyte from performance-affecting impurities such as Fe, which are, however, certainly present in the industry and create decisive differences in electrode environment. Besides, bubble removal is restricted by the rotation speed of the disc leading to a maximum current density of 100 mA cm⁻²; mostly current densities of 10 mA cm⁻² are reported.^[23] Standard experimental protocols last from minutes to few hours; longer experiments regularly cause problems with a loss of catalyst adhesion to the electrode, which ultimately leads to the termination of the experiment.^[24,25,29–30]

A less commonly employed, and comparatively less standardized option compared to RDE at a laboratory scale is a beaker cell configuration. This type of cell offers great flexibility for achieving industrial conditions due to unrestricted electrode geometries and the availability of corrosion-resistant cell materials.^[31] However, until now, various types of beaker cells exist that are rarely comparable and the conditions remain relatively mild.^[32,33]

The gap between laboratory and industrial conditions currently represents one of the major drawbacks in the development of new electrodes for AWE. New applicable testing methods are required to bridge the gap between laboratory and industry. Based on the above discussion, we herein present an advanced beaker cell setup that is able to meet industrial conditions more closely than state-of-the-art investigation tools. The electrochemical cell can run at elevated temperatures of 80 °C in 30 wt.% KOH for more than 300 h, testing electrodes at current densities of up to 1,000 mA cm⁻². To achieve such a stable setup, the first step was to investigate the stability of various reference electrodes under hot alkaline conditions. Subsequently, four electrode holders were compared, including not only concepts known from the literature, but also new in-house developed holders for an easier and

more reproducible handling. Finally, an electrochemical measurement protocol is introduced in order to unify catalyst research on AWE electrodes and, therefore, accelerate the transfer of innovative materials from the laboratory to industrial application.

Results and Discussion

Design and Handling of the Beaker Cell Setup

Within the scope of this work, an electrochemical measuring setup for AWE was developed, which enables electrode investigation under near industrial conditions (see Figure 2). The cell itself consists of a 250 mL polytetrafluoroethylene (PTFE) beaker filled up with 220 mL of 30 wt.% KOH. PTFE was chosen instead of a common glass beaker in order to avoid glass corrosion that might impact the electrocatalysts properties.^[34,35] Both working electrode (WE) and counter electrode (CE) are made of industrial standard Ni mesh with a geometrical electrode area of 1 cm² and face each other with a distance of 16.5 mm. The WE can be coated with the catalyst material to be researched. In the experiments conducted in this work, either the bare Ni mesh or industrial benchmark electrodes provided by De Nora are used. As a CE, we recommend using a Ni mesh without any catalyst coating. Both WE and CE are integrated into the system using an in-house designed Ni tuck-in holder, which is described in detail in the chapter

“Electrode Holders” (*vide infra*). As a reference electrode (RE), a Hg/HgO electrode is placed in a diagonal direction facing the lower corner of the WE with a distance of ~2 mm. This positioning allows a low resistance between RE and WE to be achieved without the need of a Luggin capillary. At the same time no bubbles are accumulated at the tip due to the inclination. The stability of various reference electrodes is also examined in more detail (“Reference Electrodes”, *vide infra*). The three electrodes are installed in a PTFE lid, which is specifically designed for the beaker cell setup and can easily be fabricated in a mechanical workshop by machining a solid PTFE round rod with a diameter of 80 mm. In addition to the openings for the three electrodes, three further openings are also provided in the lid: One central opening is used to insert a temperature sensor, whereas another opening is installed for the gas outlet. The third opening provides multifunctional options *e.g.*, taking electrolyte samples, water redosing and RE tracking. Finally, a groove is provided in the lid for the installation of an ethylene-propylene-diene-monomer (EPDM) sealing ring (63×2 mm) so that both product gas and water vapor can only escape through the opening provided for this purpose. A detailed constructive diagram of the lid can be found in the Supplementary Material (see Figure S1).

The beaker cell is placed on a magnetic stirrer with heating function. The temperature sensor is immersed ~3 cm above the bottom of the beaker, the temperature regulation is set at 80 °C, and the electrodes are slowly heated up in the electrolyte. A mild stirring rate of 100 rpm using a PTFE covered magnetic

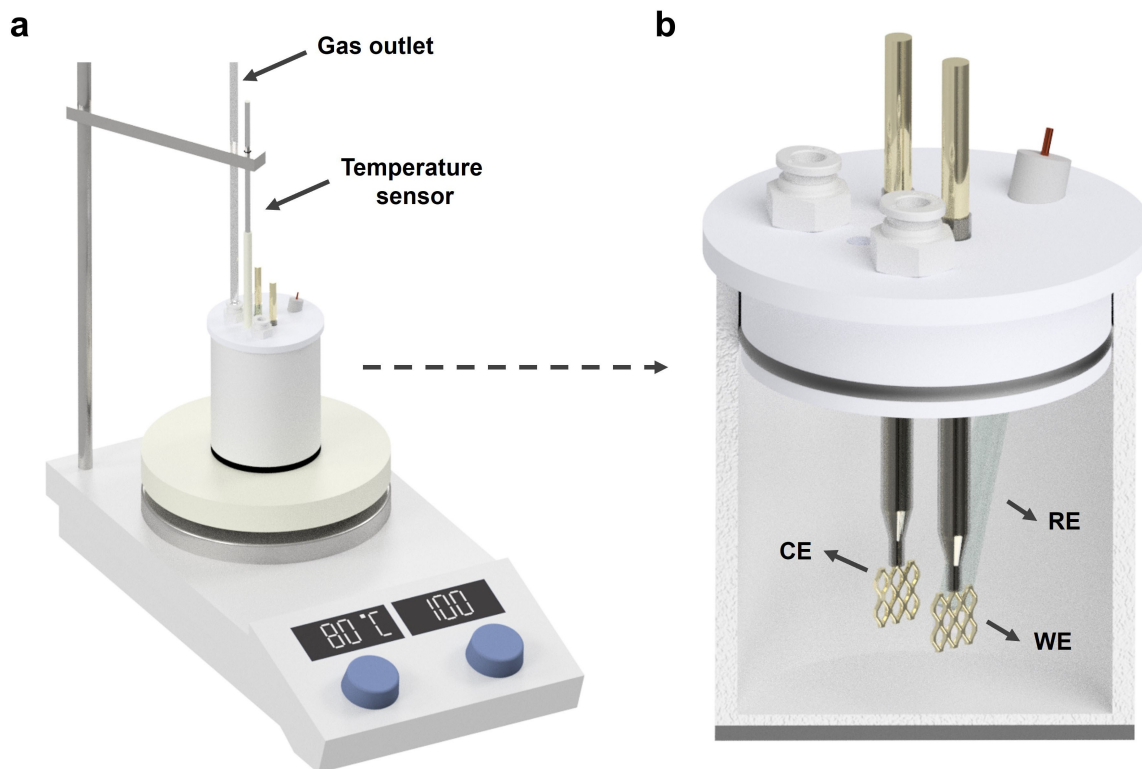


Figure 2. CAD representation of the beaker cell setup including a heated stirring plate with an external PTFE-covered temperature sensor and an exhaust pipe for the evolving O₂ and H₂ (a). Cross-section view of the beaker cell including a PTFE-beaker and -lid, the Hg/HgO RE, Ni mesh electrodes in the dimensions 1×1 cm² as the working electrode (WE), and 1×1 cm² as the counter electrode (CE). WE and CE are inserted using an in-house designed Ni tuck-in holder (b).

stirrer is recommended for an even temperature distribution in the beaker cell. Note that the temperature sensor also has to be coated by PTFE to prevent corrosion and dissolution of impurities such as Fe, which could influence the electrochemical measurement. For safe operation of the cell, sufficient dilution of the H₂ needs to be ensured by the user. We recommend implementing a long (~1 m) and thin (<4 mm) vertical exhaust tube connected to explosion-proof air ventilation, which also minimizes water losses, as water vapor can slowly condensate in the tube and flow back into the system. During the experiment, the remaining multifunctional opening can be used for RE tracking, electrolyte sampling and/or water redosing. A picture of the complete setup in the laboratory can be found in the Supplementary Material (see Figure S2).

Electrolyte

Electrolyte types, concentrations, and impurity levels significantly influence the electrochemical behavior of the electrode materials.^[36] Apart from KOH, which is commonly employed in industrial application, NaOH is frequently used in the literature when assessing the performance of novel catalyst materials.^[7,24,37] This represents a key problem in comparability of research data and we therefore highly recommend using 30 wt.% KOH when investigating catalysts for AWE.

Furthermore, we want to highlight the importance of electrolyte quality. Electrode manufacturers limit the concentration of various impurities, such as Cr, Ca, Mg, Cl, C, Si and S, as they negatively affect the performance of AWE.^[18,36] The most well-known exception in this case is the effect of Fe in solution, as it increases the initial activity of Ni and Co based anodes significantly.^[38–41] Recently, researchers therefore sometimes purify the electrolyte, in order to investigate the intrinsic performance of the catalysts without having a performance-enhancing effect of the Fe.^[42–44] While being relevant for a fundamental understanding, it defers from practical application, as some amount of Fe is certainly present in industry due to exogenous and endogenous sources.^[36] However, quantifying this amount in a general sense remains challenging. Some electrode manufacturers limit the maximum Fe concentration (e.g. <200 ppb), likely to ensure long-term stability.^[18] On the other hand, many system manufacturers utilize steel in system periphery and may not be able to adhere to these limits. Based on this discussion, we recommend conducting beaker cell experiments with significant Fe impurities (>50 ppb), but even more important, we recommend the consequent determination and indication of the Fe concentration when reporting AWE data. In this work, the Fe concentration of our 30 wt.% KOH was determined to 120 ppb using ICP-OES.

Reference Electrodes

In most catalyst studies, new electrode materials are measured in a three-electrode-setup. The potential of the electrode of interest (WE) is measured with respect to the potential of a

RE.^[45] To ensure that data on the WE are obtained reliably and reproducibly, an exceedingly stable RE is required. Therefore, choosing an appropriate RE that matches the reaction conditions is of utmost importance. Hence, the unique environment (30 wt.% KOH, 80 °C) in the beaker cell represents a considerable challenge, as it deviates significantly from standard laboratory conditions (1 M / ~5 wt.% KOH, RT) for testing.

For typical AWE experiments three types of REs have been mainly reported. The state-of-the-art RE for alkaline media is the Hg/HgO RE, as Hg is chemically stable in alkaline environments and, therefore, recommended by fundamental literature.^[46,47] As a consequence, Hg/HgO REs have been widely used with great success in numerous publications under mild conditions.^[32,40,41] In addition, this type of electrode has also been utilized in industrial hot alkali environments for short-term measurements.^[48] However, due to environmental concerns (toxic, naturally nondegradable, etc.), there have been repeated efforts in recent years to replace Hg/HgO REs by less hazardous REs in alkaline systems. For instance, a leakless Ag/AgCl has also been used most recently in 1 M KOH.^[33] This type of electrode is generally known for its use in acidic environments and is unstable in alkaline because of the formation of soluble Ag₂O with increasing pH value.^[46] Nevertheless, by applying the leakless technology using special ion-exchange membranes, it is promoted by literature and the manufacturer to be also suitable for weak alkaline environments.^[49,50] In addition to the leakless Ag/AgCl, the direct reversible hydrogen electrode (RHE) has lately been utilized in alkaline environments.^[42] Moussallem *et al.* have already implemented this type of RE in short-term experiments under hot-alkali environments (30 wt.% NaOH, 80 °C), but its stability was not described.^[51] In summary, the three types of reference electrodes were successfully implemented for measurements under laboratory conditions or short-term measurements at elevated concentrations and temperatures. However, there are only few and inconclusive reports available about the REs' stabilities under the industrial conditions aimed for in the beaker cell.

Four electrodes were selected and tested for their long-term stability under industrial conditions: A state-of-the-art Hg/HgO (ALS), a leak-free Ag/AgCl (Innovative Instruments), a regular RHE (Gaskatel), and a miniRHE (Gaskatel). The REs were immersed in 30 wt.% KOH at 80 °C for a total of 4 weeks and tracked against a master-RHE (Gaskatel) on a regular basis. To ensure the proper functionality of the master-RHE, it was measured against a true RHE on a weekly basis.^[52,53] For both the miniRHE and the regular RHE, the expected RE potentials with respect to RHE are obviously 0 mV vs. RHE. In contrast, the expected potentials for the Hg/HgO and Ag/AgCl RE are neither trivial nor well reported, as the conditions deviate greatly from the common literature in terms of temperature and pH. The RE potentials are partly based on thermodynamic calculations, but also on experimental data. Herein, multiple effects have to be accounted for such as the exact temperature dependencies, liquid junction potentials, steam partial pressures and water activities.^[47] For instance, the potentials for Ag/AgCl REs are commonly only investigated for pH 0.^[54] Thus, the potential to be expected for our conditions was estimated using the Nernst

equation (see Supplementary Material) and results in 1,114 mV vs. RHE. For the Hg/HgO, a viable option is to use the approximated equations from the study by Balej *et al.*, which results in a potential of 909 mV vs. RHE.^[48,55]

The four selected REs are examined with regard to their deviation from the literature value and, more importantly, concerning the day-to-day fluctuations reflecting the long-term stability of the electrodes (see Figure 3a&b). The Hg/HgO RE from ALS demonstrated an average potential of 916 \pm 8 mV vs. RHE, which is about 7 mV above the calculated potential of 909 mV vs. RHE.^[48] In addition, there was an initial decrease of around 7 mV in the average potential during the first 14 days, which remained significantly more stable for the following 14 days. This led to an average potential of 911 \pm 4 mV for the second half of the testing period, which is in close proximity to the reported equilibrium. As a result, the Hg/HgO REs require two weeks to stabilize under the given conditions and perform more reliably afterwards. The leakless Ag/AgCl electrode showed by far the biggest deviation considering the period of 4 weeks. In the beginning, the electrode showed a potential of 1,109 mV vs. RHE, which is 5 mV below the calculated value of 1,114 mV vs. RHE. However, between week 1 and 2, the potential of the Ag/AgCl electrode drastically decreased by more than 300 mV and then stabilized at an average potential of 791 \pm 8 mV vs. RHE for the last two weeks of the testing period. This behavior might be due to the failure of the installed membrane, which in the worst case could lead to a leakage of the contained KCl. Lastly, and unlike the Hg/HgO and the Ag/AgCl RE, the regular RHE and miniRHE show a uniform variance around the mean value for the entire testing period. However, among the two RHEs, the miniRHE performed superior in two regards. Its average potential accounts for 7 \pm 1 mV vs. RHE and, therefore, is much closer to the thermodynamic potential than the regular RHE with 19 \pm 7 mV vs. RHE. Furthermore,

the standard deviation for the miniRHE is about 7 times smaller than that of the regular RHE, and thus, the smallest of all tested reference electrodes.

In summary, the miniRHE exhibited the lowest potential variation over a 4-week period and even outperformed the state-of-the-art Hg/HgO electrode, which is also performing fairly reliably after two weeks of conditioning. Unexpectedly, and compared to the outstanding performance of miniRHE, the regular RHEs showed not only large potential variations but also fragility when used as the master-RHE, as a total of two master-RHEs lost their functionality and had to be exchanged during the course of this study. It seems that the sudden change in temperature when the electrodes are immersed in the hot KOH from ambient conditions is damaging to the RHEs. Finally, the Ag/AgCl RE, despite the leak-free technology, is unsuitable for the extreme conditions in the beaker cell. However, we would like to note that a sufficiently reliable and stable performance was obtained under mild conditions (1 M KOH, 25 °C) for a period of multiple months until the REs start to shift (see Supplementary Material Figure S3).

Electrode Holders

A major challenge when designing electrochemical cells is the integration of the WE. Herein, it is important to manufacture these precisely and reproducibly due to the particularly small active electrode areas used in laboratory tests. At the same time, however, good electrical contact must be ensured, whereby the contacting material itself should ideally be isolated from the reaction to prohibit any contribution. For the special case of the beaker cell demonstrated in this study, the harsh hot alkali conditions also complicate the choice of material for the electrode holder.

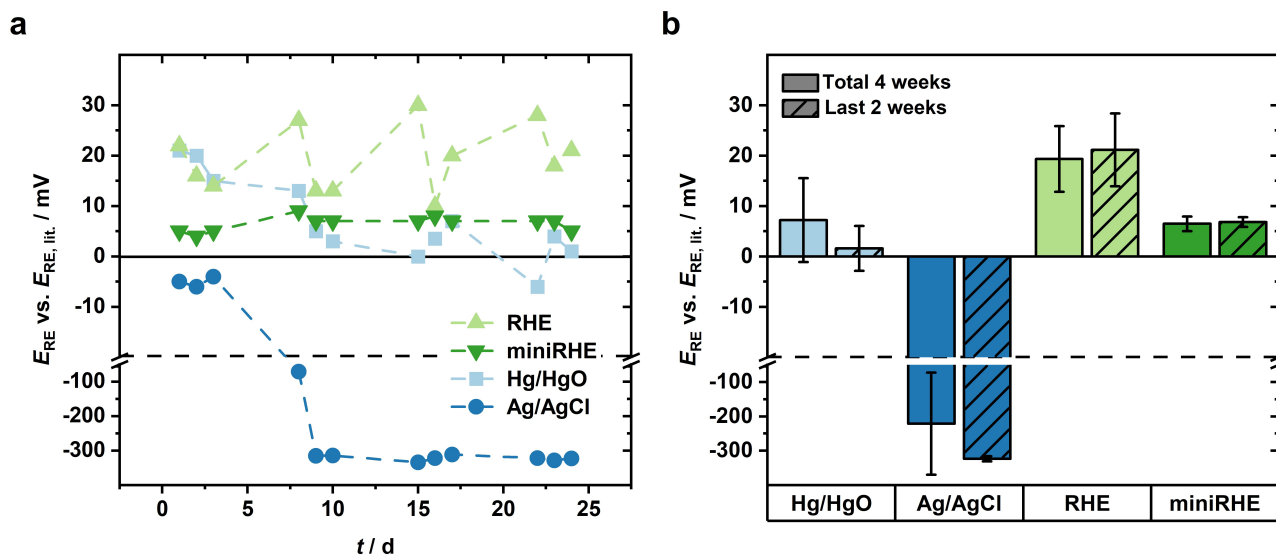


Figure 3. Detailed potential profile for different REs for a total of 4 weeks (a) and average potential including standard deviation for 4 weeks and for the last 2 weeks (b) in mV against reported literature values for a Hg/HgO (lit. value: 909 mV vs. RHE),^[48] leakless Ag/AgCl (lit. value: 1,114 mV vs. RHE),^[54] All potentials were obtained via OCP measurements against a master RHE. REs were exposed to 30 wt.% KOH at 80 °C throughout the entire time, the master-RHE was only immersed intermittently for the OCP measurement and regularly tracked against a true RHE.

As mentioned previously, the majority of the OER tests are carried out in the RDE setup. However, simple beaker cell setups under mild alkaline conditions are also used occasionally. In this case, basic electrolyte vessels are used, in which the electrodes are immersed and contacted above the electrolyte level with a clamp.^[32] The active area of the electrodes is then regulated by the immersion depth. However, one drawback of this solution is that the active area can only be determined within a relatively large margin of error, as the electrolyte spreads above the electrolyte level due to capillary forces. In addition, the electrolyte volume must be kept constant; otherwise, the active area will shrink during the course of the experiment. As a result, long-term experiments and a temperature increase with such an electrode holder are not recommended, since minimal evaporation has a significant effect on the active electrode area. To overcome these drawbacks and to limit the electrode area more reliably, some authors use hot glue or epoxy resin to seal electrode area, that is not supposed to impact the reaction.^[9,33] The electrodes are then intentionally immersed a little deeper in the electrolyte so that electrolyte evaporation and consumption does not directly impact the active area. So far, this method has only been tested under mild conditions. Verification under industrial conditions is still lacking, where the possibility of impurity release from the glues would need to be investigated. Furthermore, this method is very laborious, as new electrodes must be embedded repeatedly for every experiment and have to be significantly larger than the actual active area.

Up to now, academia only uses holders that either provide short-term and inaccurate results or are complicated to handle. Furthermore, verification of the holder's functionality under hot alkaline conditions is still completely lacking. Therefore, within this work, four holders were compared with respect to suitability under industrial conditions. Figure 4a shows the simplest holder, which is also commercially available (DEK Research). Here, the electrode is sandwiched between the PTFE corpus and a Pt plate for electrical connection and then fully immersed in the electrolyte. Figure 4b shows a soldered

electrode holder, in which the electrode is soldered with Zn to a Ni rod at the top part and the excess surface is sealed with PTFE tubing and tape. The third holder is designed to be industry-oriented, as it is a welded holder, where, similar to the soldered holder, the electrodes are connected with a Ni rod and then sealed with PTFE (Figure 4c). The last method is a Ni tuck-in holder, where the electrode is fixed at the upper end in a tapered hole in a Ni rod. The remaining excess surface is also sealed here with PTFE tubing and PTFE tape (Figure 4d). A CAD construction image of the holder is given in the Supplementary Material (Figure S4). Pictures of the real electrode holders from the laboratory can be found in the Supplementary Material as well (Figure S5). The four holders were compared by installing the De Nora industrial benchmark electrodes (expanded metal mesh) in all electrode holders. Herein, it is particularly important that when the mesh is cut to size, a bar remains above the active electrode area of 1 cm², which is about 1 cm long and is then pressed together. This bar can then be used for soldering, welding, or tucking.

The evaluation of electrode holders involves assessing their performance based on several criteria, including the activity and its reproducibility, the level of measurement noise, the uncompensated resistance, and the long-term stability of the benchmark electrodes installed in the holders. All data was generated using the electrochemical protocol introduced in the chapter "Protocol-Recommendation" (*vide infra*). At least 3 repetitions using new WEs were carried out for each holder. The initial electrode activity, which was recorded using stationary polarization, is shown in Figure 5a for the four holders. Herein, the worst activity and reproducibility was observed with the commercial electrode holder, in which the benchmark electrode from De Nora represented a potential of 1,598 ± 7 mV vs. RHE at a current density of 1,000 mA cm⁻². The remaining three electrode holders perform much better in terms of activity and reproducibility, with the welded holder (1,568 ± 3 mV vs. RHE) slightly outperforming the Ni tuck-in holder (1,573 ± 4 mV vs. RHE), which in turn slightly outperforms the soldered electrode holder (1,580 ± 3 mV vs. RHE). The poor activity of the electrode in commercial holders is likely attributed to the overly generic design of the holder, as the electrode is clamped between the two PTFE bodies and accumulates gas over time at the top of the electrode. As a result, the active electrode area decreases abruptly, resulting in a loss of activity. The commercial holder's issue with gas bubble removal can also be observed in Figure 5b, where the holder exhibits significant noise, particularly at higher current densities of 500 and 1,000 mA cm⁻². This indicates that larger gas bubbles repeatedly accumulate on the holder within a few seconds, restricting the active electrode surface and subsequently detach. In contrast, all three other holders do not exhibit this characteristic, as they are specifically designed for the use of porous electrodes such as expanded meshes. The simplistic design of the commercial holder is also responsible for its poor reproducibility (see Figure 5a). It is challenging to consistently position the electrode in the same manner within the holder and exerting persistent pressure with the screw for electrical contact. The difficulty of achieving consistent electrical contact

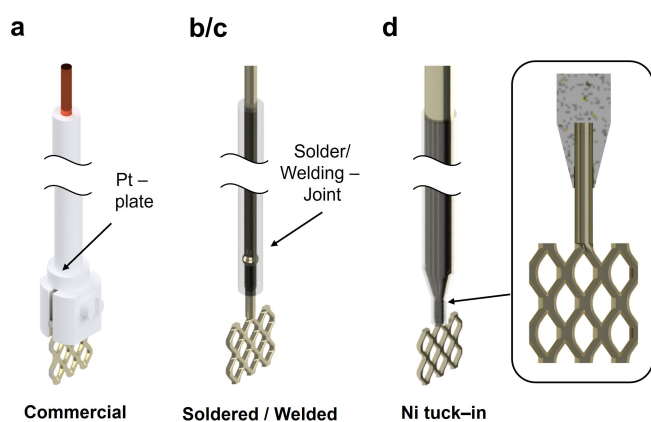


Figure 4. CAD representation of the four holders investigated: Commercial electrode holder (a), electrode soldered/welded to a Ni rod and PTFE sealed (b/c), electrode build in an in-house designed Ni tuck-in holder and sealed with PTFE (d).

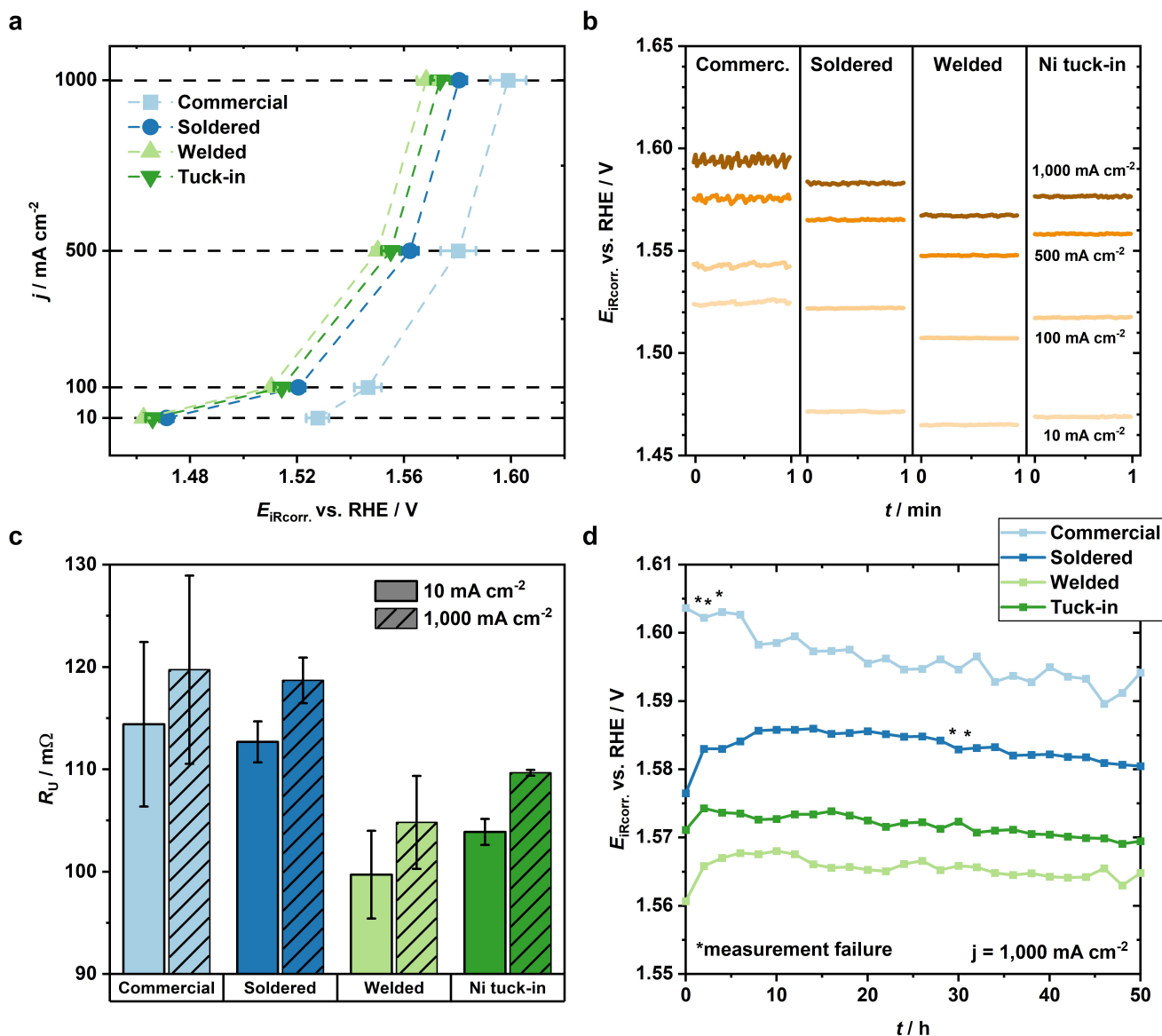


Figure 5. Stationary polarization with data points at 10, 100, 500, and 1,000 mA cm⁻² (a), chronopotentiometric steps of 10, 100, 500, and 1,000 mA cm⁻² for 1 min each (b), uncompensated resistance (R_u) measured via EIS at 10 and 1,000 A cm⁻² (c), and chronopotentiometry at 1,000 mA cm⁻² for 50 h (d) shown for the commercial, the soldered, the welded and the Ni tuck-in electrode holder.

through screw pressure can also be observed in Figure 5c. Herein, the commercial holder not only displays the highest uncompensated resistance, but also the largest deviation (120 ± 13 mΩ), underlining its issue with reproducibility.

Despite the lacking suitability of the commercial holder, there is still an observable difference concerning the electrodes activity between the remaining three holders, which is not easily explained. Herein, the welded holder performed better than the Ni tuck-in holder, which, in turn, performed better than the soldered one. Interestingly, although the electrode holders are arranged in the same manner in the cell, the welded holder exhibits the lowest ohmic resistance of 105 ± 6 mΩ, the Ni tuck-in holder 110 mΩ, and the soldered holder 119 ± 4 mΩ. Thus, when comparing the activity and uncompensated resistance, it appears that electrode holders with

higher resistance also exhibit poorer activity, even though the activity is displayed with 100% iR -corrected potentials, which in theory is intended to eliminate the influence of electrical contact. This discrepancy shall be investigated in more detail in a follow-up study.

In addition to the short-term activity tests, the influence of the holders on the long-term stability of the benchmark electrodes was also examined over a period of 50 h. Herein, despite the already discussed difference in initial activity, all holders show a decreasing potential, which is likely related to the increasing concentration of KOH due to water consumption. Interestingly, the concentration increase is not displayed in the uncompensated resistance, which stays relatively constant (see Supplementary Material Figure S6). The reduction of the overpotential therefore seems to be impacted by the local environ-

ment of the electrode, presumably the increase of the pH value. In addition to the reduction of overpotential, it was found that both the commercial holder and the soldered holder experienced several experiment failures during this time. While the commercial holder exhibited failures mostly at the beginning due to faulty contact, two soldered holders failed abruptly after several hours of measurement. The latter was attributed to the dissolution of soldering tin, suggesting that if the seal with PTFE is not perfectly tight, the incoming KOH acts highly corrosive on the soldering material.

From a pure measurement performance standpoint, the industry-inspired welded holder appears to be the best option in terms of activity, reproducibility, and reliability. However, this holder comes with some drawbacks from an application perspective. On the one hand, welding such small Ni connections is challenging and hence often beyond the capabilities of many laboratories. Furthermore, the high temperatures involved in welding pose extreme conditions for the electrode and might alter the structure of the catalyst. In contrast, the in-house designed Ni tuck-in holder is much easier to handle and requires a total of 5 min, including sealing, for experiment preparation. Taking this into account, the slightly worse activity achieved with the tuck-in holder can be tolerated in exchange for the better applicability. Therefore, the in-house designed Ni tuck-in holder is recommended for everyday laboratory needs.

Long-Term Measurements

A crucial factor for AWE industry in choosing electrode materials is their long-term stability. The electrode systems should be particularly low-maintenance, i.e. designed for use of more than 5 years, and should lose little performance during this time, as the energy costs make up a large part of the hydrogen production costs.^[18] Nevertheless, academia has conducted limited research on the stability of electrode materials, in particular for technically relevant conditions. As for these conditions nowadays only complex and hence expensive flow-cell test rigs can be used, long-term experiments are rather scarce due to capacity bottlenecks. The long-term measurement of electrode materials in the beaker cell could therefore be a simple and cost-effective alternative.

However, the challenge here is to keep the electrolyte concentration constant despite the conversion of water and possible evaporation. The theoretical water loss due to electrochemical conversion can be calculated with the help of Faraday's law according to Eq. 1.

$$\dot{V} = 0.336 \frac{\text{mL}}{\text{h} \cdot \text{A}} \cdot I \quad (1)$$

From this, it follows that in an experiment over 300 h at $1,000 \text{ mA cm}^{-2}$, about 100 mL of water is converted, which is approximately 46% of the total beaker content. One way to lessen this issue would be to increase beaker volumes, however this again leads to more cost and complexity in the lab. Given

this background, regular re-dosing of water is vital for providing a stable environment and therefore, receiving reliable data.

Figure 6 shows a long-term measurement over 300 h of the De Nora benchmark electrode. During the entire test period, water was added at regular intervals a total of 5 times. It can be clearly seen that the maximum potential of 1.58 V vs. RHE is reached at the beginning of the experiment and is recovered immediately after the redosing of water. After this, a slight decrease in potential is always observed, with a slope of 0.2 mV h^{-1} . Therefore, it appears that the industrially used benchmark electrode is highly stable and already fully conditioned, and the feigned activation of the electrode is actually a result of increasing electrolyte concentration due to water conversion.

The amount of additional water that had to be added in the beaker during the experiment corresponded perfectly to the theoretical conversion amount, resulting from Eq.1. Significant losses due to evaporation can therefore be neglected, since a thin and long exhaust tube was used, in which the steam could condense and run back in the beaker (*vide supra*). Nevertheless, if monitoring the electrolyte level visually is desired, we recommend using a strong light source, which makes the PTFE beaker slightly transparent.

Protocol-Recommendation

As the beaker cell presented in this work fulfils the industrial conditions, provides reproducible results and is easy to handle in the laboratory, it is well-suited for benchmarking new electrode materials. To this end, a new harmonized electrochemical testing protocol is recommended in the following, that can be applied by the respective users. A schematic overview is shown in Figure 7, comprising the three main sections of the protocol namely conditioning, activity measurement and the stressor. Herein, an essential part is the activity measurement, i.e. the correlation between current and voltage

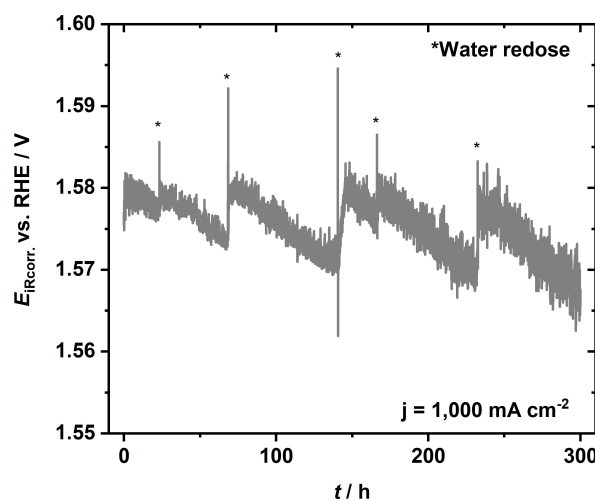


Figure 6. Chronopotentiometry at $1,000 \text{ mA cm}^{-2}$ of De Nora benchmark electrode for 300 h. Stars indicate water redosing according to theoretical water consumption.

for the respective material. In literature, most activity measurements are carried out using cyclic voltammetry in a defined potential range. However, for reasons of reproducibility, stationary polarization was lately recommended for the activity measurements, since it eliminates non-faradaic effects and characterizes the electrode in a stable operating environment.^[33] Therefore, results obtained from stationary polarization measurement were chosen as an activity indicator for this protocol, too. In addition to the initial electrode activity, the stability of the electrode needs to be characterized, as it is of utmost importance for industry. Since the state-of-the-art three-electrode setups may only provide limited understanding of it, the stability of many materials is not studied and if so, sophisticated flow-cell tests have to be carried out for the most promising materials. As mentioned previously, chronopotentiometry may then be chosen as an electrochemical technique, which represents the use of constant load as a stressor (i.e. fossil fuels or nuclear energy). However, the latest studies recommend the use of a dynamic load, since alkaline water electrolysis is intended for coupling with renewable energies. In order to simulate a long operating time of the electrolyzer with a correspondingly large number of load changes, accelerated stress tests (ASTs) have been developed, in which the load is changed from full to low load every minute.^[56] These ASTs are shown as the second stressor option (alternating load) recommended for benchmarking electrode materials in the beaker cell. During the experiment, the stability measurement is interrupted for an activity measurement every 2 h, meaning that activity and stability are repeated alternately. This allows for describing the performance of the electrode (activity) at a given time throughout the entire current range while operating the electrode independently at a selected operating point (stressor). Significant statements about the status of the electrodes can then be made by comparing the activity measurements at different points along the measurement.

In detail, the first section of the protocol, the conditioning, starts off with measuring the open circuit potential (OCP) for 2 h (see Figure 7a). This serves to adjust the temperature of 80 °C in the beaker and at the same time to chemically precondition the materials to be examined under industrial conditions. Once a stable temperature of 80 °C has been reached, the RE can be tracked with the help of another master-RE (e.g. miniRHE from Gaskatel). We recommend that the master electrode used is also regularly tracked against a true RHE.^[52,53] Afterwards, the electrode can also be further electrochemically conditioned by cyclic voltammetry. However, the technique's parameters must be adapted to the respective electrode material and manufacturing method, which is why no exact methodology is recommended within the scope of this protocol. Once conditioning is complete, the main part of the protocol consists of recurring the activity measurement and the selected stressor. A tabular presentation of the protocol can be found in the Supplementary Material (see Table S1).

A single activity measurement consists of several current steps (e.g. 10, 100, 500 and 1,000 mA cm⁻²) for 3 min each that add up to a stationary polarization of the electrode material (see Figure 7b). We recommend averaging the last minute to a

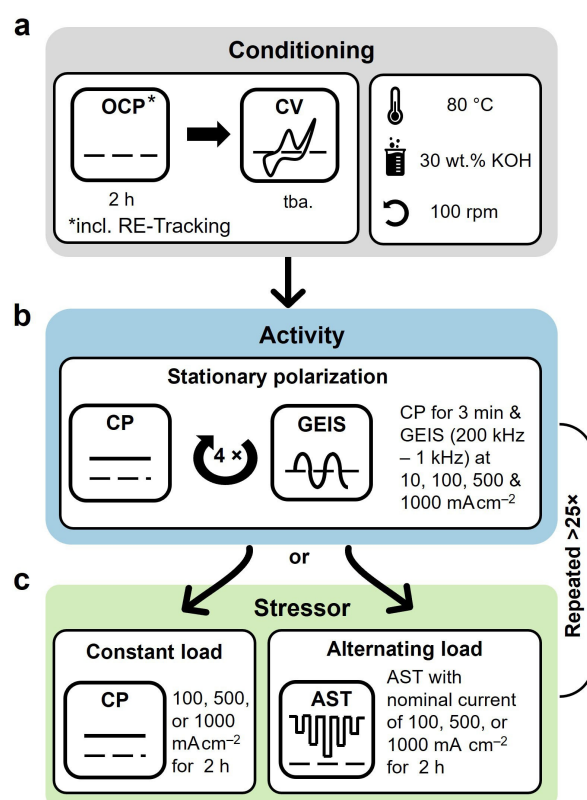


Figure 7. Schematic overview of the proposed measurement protocol for benchmarking OER electrodes under industry-relevant conditions in the beaker cell. The protocol consists of a conditioning step (a) followed by recurring activity (b) and stressor (c) steps. As stressors, one can either choose a constant load or an alternating load.

data point at each current. Further current densities can also be added, however, the proposed current densities of 10, 100, 500 and 1,000 mA cm⁻² are well-suited to work as benchmark current densities that may be used for intra-lab comparability. Note, if the existing potentiostat hardware does not provide the highest currents, measurements should be taken through all possible benchmarking currents and then additionally up to the highest possible current density, that the potentiostat can provide. As an example, 10, 100 and 400 mA cm⁻² may be measured, if the potentiostat can only provide a maximum current density of 400 mA cm⁻². All steps are followed by galvanostatic electrochemical impedance spectroscopy (GEIS) at the respective operating values and interconnected by galvanodynamic elements with a slope of 10 mA cm⁻² s⁻¹ (see Figure 8a).

For measuring stability, two different stressors can be selected, depending on the targeted application (see Figure 7c). The first option stresses the electrode by applying a CP of preferably 1,000 mA cm⁻². However, at an earlier stage of electrode development or if limited by the potentiostat, a lower current of 100 or 500 mA cm⁻² may be applied. Once again, 100, 500 & 1,000 mA cm⁻² may serve as benchmarking current densities for comparability reason and it is advised to measure these in consecutive experiments, given that the potentiostat provides the power needed. As the second option for aging the

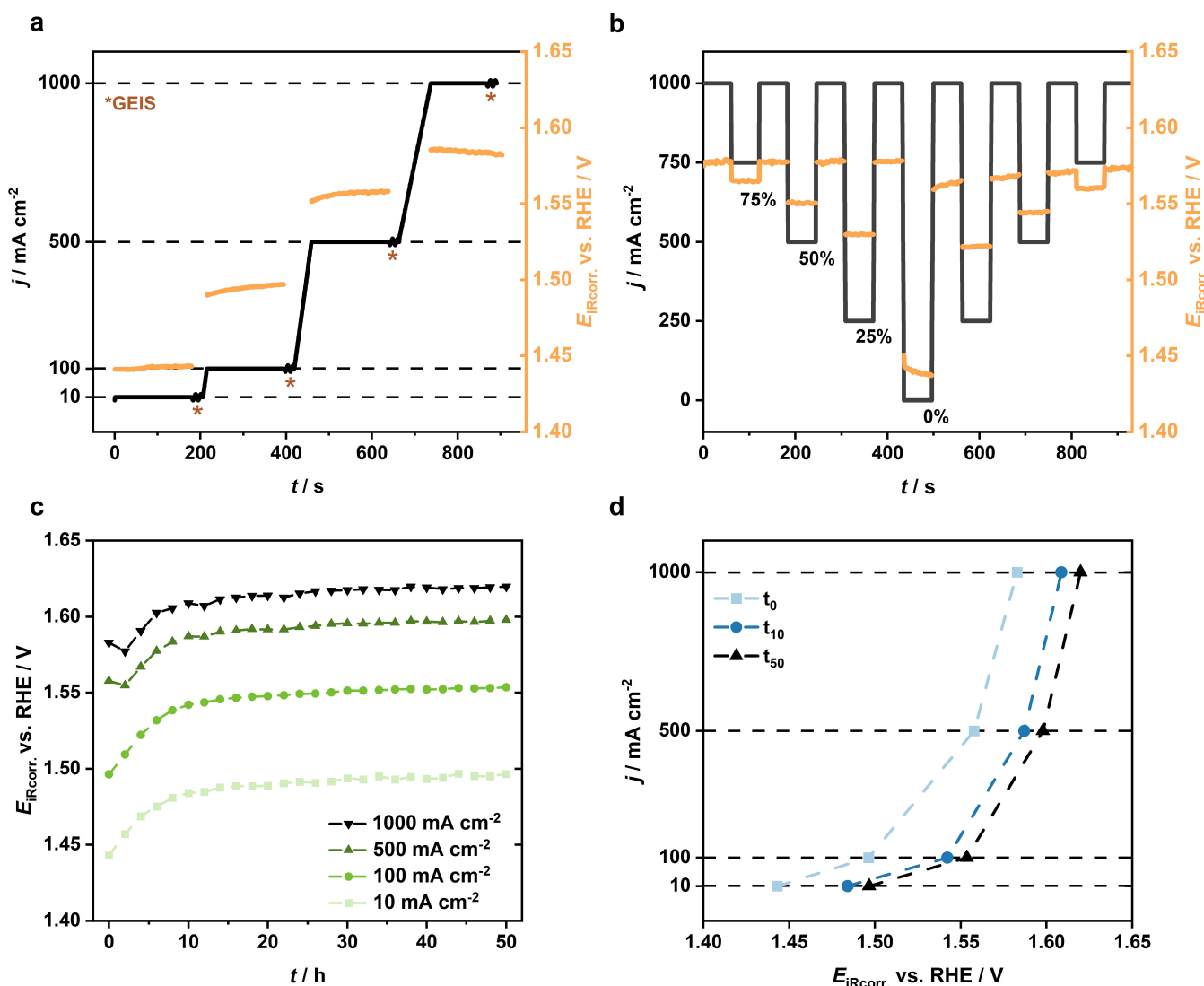


Figure 8. (a) Detailed presentation of the proposed activity measurement in the form of a stationary polarization and the responding potential for a Ni mesh. Chronopotentiometry is measured for 3 min followed by GEIS for current densities of 10, 100, 500, and 1,000 mA cm⁻². The individual currents are reached with a slope of 10 mA cm⁻² s⁻¹. (b) Detailed presentation of proposed AST with a nominal current of 1,000 mA cm⁻² and the corresponding potential. (c) All 26 activity measurements displayed for 10, 100, 500, and 1,000 mA cm⁻². Data points represent the mean value of the last 60 s of the stationary polarization at each current. (d) Comparison of stationary polarization curves obtained for a Ni mesh at $t=0$ h, $t=10$ h and $t=50$ h.

electrode, ASTs according to Tsofidris *et al.* are recommended.^[56] Herein, current steps between the nominal value of either 100, 500 or 1,000 mA cm⁻², which represent 100% load and partial load ranges of 75%, 50%, 25% and shut-down are iterated for 1 min each and connected *via* galvanodynamic elements with a slope of 250 mA cm⁻² s⁻¹ (see Figure 8b). The displayed pattern is then repeated 8 times, which sums up to ~2 h. Interestingly, for the chosen Ni electrode, the received potential at 0 mA cm⁻² is ~1.44 V vs. RHE, which is still significantly above the open circuit potential. Thus, the ASTs from Tsofidris *et al.* do not simulate a real shut-down of an electrolyzer, but rather investigate the stability under dynamic load cycles without reducing the electrode's surface.^[56–58] Therefore, it could be interesting to investigate the stability by setting a lower potential and intentionally force the reduction of the electrode, *e.g.* according to Haleem *et al.*^[59] Furthermore,

another option for stress-testing the materials could involve applying even higher current densities.

In the course of the experiment, the activity measurement and the selected stressor are repeated alternately until the total duration is at least 50 h (25 repetitions), *i.e.*, a total of 26 activity measurements are available. We consider a 50-hour measurement (approximately 2 days) to offer a favorable balance between effort and insights into the electrode's performance, but every user can further extend the measurement according to the stage of electrode development. The stability of the respective electrode material can now be evaluated by comparing the activity measurements over time. Figure 8c shows all 26 activity measurements for a Ni mesh altered with AST, with the respective data points indicating the average potential of the last 60 s of the current steps of stationary polarization. Note that the Ni mesh was preconditioned using

50 CV cycles with a scan rate of 100 mV s^{-1} in the range of 0.2–1.55 V vs. RHE. Figure 8d provides a different representation of the degradation of the electrode by showing selected polarization curves at the beginning, after 10 h and at the end of the test after 50 h. Unlike the De Nora benchmark electrode, which was used for the rest of this work, the comparison of the industrial standard Ni mesh reveals a total degradation of $\sim 50 \text{ mV}$ for the entire current range.

Conclusions

In summary, a new setup and the corresponding measurement procedure were developed that can conduct laboratory-scale tests on AWE electrode materials under industrially relevant conditions. The herein reported beaker cell is able to reproducibly conduct measurements at 80°C in 30 wt.% KOH for more than 300 hours, while being affordable and easy in handling compared to tests in flow-cell setups. As a RE, both Hg/HgO and a miniRHE proved to be suitable in the harsh environment, whereby the miniRHE showed extraordinary stability of $7 \pm 1 \text{ mV}$ vs. RHE over the 4-week test period. Furthermore, several electrode holders were investigated for the reproducible and efficient installation of the electrodes, whereby an in-house designed Ni tuck-in holder proved to be the best option in terms of handling and performance (activity and reproducibility), providing a potential of $1,573 \pm 4 \text{ mV}$ vs. RHE at $1,000 \text{ mA cm}^{-2}$ for the industrial benchmark electrode. To promote an inter-lab comparability of beaker cell tests, an industry-oriented electrochemical measurement protocol was introduced, so that the beaker cell can be used as a benchmarking tool for future research. In this way, the work presented herein contributes to ensuring that new electrode materials developed in the laboratory are more likely to translate into industry innovation. Further investigations to translate the beaker cell results to an electrolyzer flow-cell are currently in progress.

Experimental Section

As this work primarily focuses on a new measurement methodology, the actual experimental procedure is extensively discussed in the preceding chapters: “Design and Handling of the Beaker Cell Setup” and “Protocol Recommendation” (*vide supra*). Here we describe additionally the materials and chemicals used, if not stated in the main chapters.

For the beaker cell setup, an AREX 6 Digital PRO hot plate from Velp Scientifica was used and the stainless-steel thermocouple was rigorously covered with PTFE tape (Bohlender). A 250 mL Thermo-tech®-PTFE beaker from VWR International and a PTFE lid according to Figure S1 was utilized. To complete the lid, an EPDM sealing ring (63×2 mm), two 4/6 mm G 1/8" IQS-connectors, and a PTFE tube (4/6 mm) for exhaust were obtained from Landefeld. DSA[®] A1 benchmark electrodes and industry-standard Ni mesh, both supplied by industry partner DeNora, were used as anode and cathode, respectively. To create the Ni tuck-in holders, Ni rods with a 5 mm diameter were purchased from HMW Hauner (99.99+%) and machined in the mechanical workshop according to Figure S4. Both

the soldered and the welded electrode holders were processed using Ni rods with a diameter of 2 mm (HMW Hauner), which were then connected to the electrode and covered with PTFE tube and tape. For the soldering process, the soldering tin (Lux Tools, 98+%) was melted using a temperature of 500°C . The welded electrodes were manufactured using the “Tungsten inert gas welding” (TIG) technique with local temperatures above $3,500^\circ\text{C}$. The beaker was filled with pre-mixed 30 wt.% KOH (Bernd Kraft) providing an overall Fe concentration of $\sim 120 \text{ ppb}$ (ICP-OES). KOH was exclusively stored and prepared in polymer-equipment (polypropylene) in order to eliminate impurities leaching from standard glassware. A VSP-300 potentiostat from Bio-Logic SAS and the accompanying EC-Lab V11.43 software from the same provider was used to apply and implement the electrochemical protocol.

Experiments for investigating the stability of various reference electrodes were also conducted in a beaker cell. All four reference electrodes were installed in the same beaker cell using a sealing lid that prevented evaporation of the electrolyte and were measured against a master RHE three times a week for a total period of four weeks. The cell and the electrodes were continuously exposed to industrial conditions (30 wt.% KOH, 80°C), while the master-RHE was only introduced into the cell for a short measurement period. The reported values were obtained from the final value of a 20-minute OCP measurement. To ensure the proper functionality of the master RHE, it was measured against a true RHE, according to Jerkiewicz *et al.*, on a weekly basis.^[52] The Hg/HgO RE was bought from ALS Co. Ltd, regular RHE and mini RHE were supplied by Gaskatel, and the leakless Ag/AgCl RE was purchased from Innovative Instruments.

Author Contributions

Conceptualization: NT, JH, DV, NS, SH, BE, AM; Data Curation: NT, ST, DV, JT, SK; Formal Analysis: NT, AM; Funding acquisition: AM, SH, BE; Investigation: NT, ST, JT, SK; Methodology: NT, DV, JT, SK; Project Administration: AM, BE; Supervision: AM, NT, BE; Validation: JH, NS; Visualization: NT; Writing-original draft: NT; Writing – review & editing: AM, ST, BE

Acknowledgements

We acknowledge financial support by the German Federal Ministry of Education and Research (BMBF project “Prometh2eus”, FKZ 03HY105A, 03HY105E & 03HY105N). Furthermore, we thank our industry partner De Nora, particularly Dr. Praveen V. Narangoda, Dr. Emanuele Instuli and Dr. Robert Scannell for providing electrode materials and guiding us through this project. Open Access funding enabled and organized by Projekt DEAL.

Conflict of Interests

The authors declare no conflict of interest.

Data Availability Statement

The data that support the findings of this study are available from the corresponding author upon reasonable request.

Keywords: Alkaline Water Electrolysis · Benchmarking · Cell Development · Industrial Chemistry · Water splitting

- [1] W. W. Clark II, J. Rifkin, *Energy Policy* **2006**, *34*, 2630–2639.
- [2] A. M. Oliveira, R. R. Beswick, Y. Yan, *Curr. Opin. Chem. Eng.* **2021**, *33*, 100701.
- [3] Y. Guo, G. Li, J. Zhou, Y. Liu, in *IOP Conference Series: Earth and Environmental Science*, Vol. 371, IOP Publishing, **2019**, p. 042022.
- [4] M. Schalenbach, *Int. J. Electrochem. Sci.* **2018**, *13*, 1173–1226.
- [5] A. Eftekhari, *Mater. Today Energy* **2017**, *5*, 37–57.
- [6] M. R. Domalanta, J. N. Bamba, D. D. Matienzo, J. A. Del Rosario-Paragguia, *J. Ocon, ChemSusChem* **2023**, *16*, e202300310.
- [7] F. Lu, M. Zhou, Y. Zhou, X. Zeng, *Small* **2017**, *13*, 1701931.
- [8] X. Xu, F. Song, X. Hu, *Nat. Commun.* **2016**, *7*, 12324.
- [9] C. Feng, F. Wang, Z. Liu, M. Nakabayashi, Y. Xiao, Q. Zeng, J. Fu, Q. Wu, C. Cui, Y. Han, N. Shibata, K. Domen, I. D. Sharp, Y. Li, *Nat. Commun.* **2021**, *12*, 5980.
- [10] B. Zhang, X. Zheng, O. Voznyy, R. Comin, M. Bajdich, M. Garcia-Melchor, L. Han, J. Xu, M. Liu, L. Zheng, *Science* **2016**, *352*, 333–337.
- [11] J. C. Ehlers, A. A. Feidenhans'l, K. T. Therkildsen, G. O. Larrazabal, *ACS Energy Lett.* **2023**, *8*, 1502–1509.
- [12] D. Siegmund, S. Metz, V. Peinecke, T. E. Warner, C. Cremers, A. Greve, T. Smolinka, D. Segets, U. P. Apfel, *JACS Au* **2021**, *1*, 527–535.
- [13] D. Zhang, K. Zeng, *Ind. Eng. Chem. Res.* **2012**, *51*, 13825–13832.
- [14] C. Karacan, F. P. Lohmann-Richters, G. P. Keeley, F. Scheepers, M. Shviro, M. Müller, M. Carmo, D. Stolten, *Int. J. Hydrogen Energy* **2022**, *47*, 4294–4303.
- [15] K. Zeng, D. Zhang, *Prog. Energy Combust. Sci.* **2010**, *36*, 307–326.
- [16] M. Carmo, D. L. Fritz, J. Mergel, D. Stolten, *Int. J. Hydrogen Energy* **2013**, *38*, 4901–4934.
- [17] D. Pletcher, F. C. Walsh, *Industrial electrochemistry*, Springer Science & Business Media, **2012**.
- [18] I. D. N. S.p.A., Electrode Package Brochure Industrie De Nora www.denora.com/applications/H2-production-by-water-electrolysis.html, **2016**.
- [19] W. Ju, M. V. F. Heinz, L. Pusterla, M. Hofer, B. Fumey, R. Castiglioni, M. Pagani, C. Battaglia, U. F. Vogt, *ACS Sustainable Chem. Eng.* **2018**, *6*, 4829–4837.
- [20] A. N. Colli, H. H. Girault, A. Battistel, *Materials* **2019**, *12*, 1336.
- [21] W.-B. Han, I.-S. Kim, M. Kim, W. C. Cho, S.-K. Kim, J. H. Joo, Y.-W. Lee, Y. Cho, H.-S. Cho, C.-H. Kim, *Electrochim. Acta* **2021**, *386*, 138458.
- [22] M. Schalenbach, O. Kasian, K. J. J. Mayrhofer, *Int. J. Hydrogen Energy* **2018**, *43*, 11932–11938.
- [23] T. Lazaridis, B. M. Stühmeier, H. A. Gasteiger, H. A. El-Sayed, *Nat. Catal.* **2022**, *5*, 363–373.
- [24] C. C. McCrory, S. Jung, I. M. Ferrer, S. M. Chatman, J. C. Peters, T. F. Jaramillo, *J. Am. Chem. Soc.* **2015**, *137*, 4347–4357.
- [25] C. C. L. McCrory, S. Jung, J. C. Peters, T. F. Jaramillo, *J. Am. Chem. Soc.* **2013**, *135*, 16977–16987.
- [26] D. D. Matienzo, T. Kutlusoy, S. Divanis, C. Bari, E. Instuli, *Catalysts* **2020**, *10*, 1387.
- [27] S. Bhandari, P. V. Narangoda, S. O. Mogensen, M. F. Tesch, A. K. Mechler, *ChemElectroChem* **2022**, *9*, e202200479.
- [28] M. F. Tesch, S. Neugebauer, P. V. Narangoda, R. Schlögl, A. K. Mechler, *RSC Energy Adv.* **2023**, *2*, 1823–1830.
- [29] H. A. El-Sayed, A. Weiß, L. F. Olbrich, G. P. Putro, H. A. Gasteiger, *J. Electrochem. Soc.* **2019**, *166*, F458–F464.
- [30] A. Hartig-Weiss, M. F. Tovini, H. A. Gasteiger, H. A. El-Sayed, *ACS Appl. Energ. Mater.* **2020**, *3*, 10323–10327.
- [31] D. D. Matienzo, D. Settipani, E. Instuli, T. Kallio, *Catalysts* **2020**, *10*, 92.
- [32] H. Zhou, F. Yu, Q. Zhu, J. Sun, F. Qin, L. Yu, J. Bao, Y. Yu, S. Chen, Z. Ren, *Energy Environ. Sci.* **2018**, *11*, 2858–2864.
- [33] A. Peugeot, C. E. Creissen, D. Karapinar, H. N. Tran, M. Schreiber, M. Fontecave, *Joule* **2021**, *5*, 1281–1300.
- [34] K. Mayrhofer, G. Wiberg, M. Arenz, *J. Electrochem. Soc.* **2007**, *155*, P1.
- [35] K. J. J. Mayrhofer, A. S. Crampton, G. K. H. Wiberg, M. Arenz, *J. Electrochem. Soc.* **2008**, *155*, P78.
- [36] H. Becker, J. Murawski, D. V. Shinde, I. E. L. Stephens, G. Hinds, G. Smith, *Sustain. Energy Fuels* **2023**, *7*, 1565–1603.
- [37] S. Jung, C. C. L. McCrory, I. M. Ferrer, J. C. Peters, T. F. Jaramillo, *J. Mater. Chem. A* **2016**, *4*, 3068–3076.
- [38] I. Spanos, J. Masa, A. Zeradjanin, R. Schlögl, *Catal. Lett.* **2021**, *151*, 1843–1856.
- [39] D. Y. Chung, P. P. Lopes, P. Farinazzo Bergamo Dias Martins, H. He, T. Kawaguchi, P. Zapol, H. You, D. Tripkovic, D. Strmcnik, Y. Zhu, S. Seifert, S. Lee, V. R. Stamenkovic, N. M. Markovic, *Nat. Energy* **2020**, *5*, 222–230.
- [40] L. Trotochaud, S. L. Young, J. K. Ranney, S. W. Boettcher, *J. Am. Chem. Soc.* **2014**, *136*, 6744–6753.
- [41] F. Bao, E. Kemppainen, I. Dorbandt, F. Xi, R. Bors, N. Maticic, R. Wenisch, R. Bagacki, C. Schary, U. Michalczik, P. Bogdanoff, I. Laueremann, R. van de Krol, R. Schlätmann, S. Calnan, *ACS Catal.* **2021**, *11*, 10537–10552.
- [42] S. Drespe, F. Dionigi, M. Klingenhof, T. Merzdorf, H. Schmies, J. Drnc, A. Poulain, P. Strasser, *ACS Catal.* **2021**, *11*, 6800–6809.
- [43] I. Spanos, M. F. Tesch, M. Yu, H. Tüysüz, J. Zhang, X. Feng, K. Müllen, R. Schlögl, A. K. Mechler, *ACS Catal.* **2019**, *9*, 8165–8170.
- [44] R. A. Márquez, K. Kawashima, Y. J. Son, G. Castelino, N. Miller, L. A. Smith, C. E. Chukwunke, C. B. Mullins, *ACS Energy Lett.* **2023**, *8*, 1141–1146.
- [45] A. J. Bard, L. R. Faulkner, *Electrochem. Meth.* **2001**, *2*, 580–632.
- [46] G. Murphy, *Science* **1966**, *154*, 1537–1537.
- [47] G. Inzelt, A. Lewenstam, F. Scholz, *Handbook of reference electrodes*, Vol. 541, Springer, **2013**.
- [48] J. Balej, *Int. J. Hydrogen Energy* **1985**, *10*, 365–374.
- [49] e. P. Ltd, eDAQ Leakless Miniature Ag-AgCl Reference Electrode, **2023**.
- [50] N. L. Walker, J. E. Dick, *Anal. Chem.* **2021**, *93*, 10065–10074.
- [51] I. Moussallem, S. Pinnow, N. Wagner, T. Turek, *Chem. Eng. Process.* **2012**, *52*, 125–131.
- [52] G. Jerkiewicz, *ACS Catal.* **2020**, *10*, 8409–8417.
- [53] S. Niu, S. Li, Y. Du, X. Han, P. Xu, *ACS Energy Lett.* **2020**, *5*, 1083–1087.
- [54] S. Meisberger, Xylem Analytics Germany Sales GmbH & Co. KG & Sensortechnik Meinsberg, **2023**.
- [55] J. N. Hausmann, B. Traynor, R. J. Myers, M. Driess, P. W. Menezes, *ACS Energy Lett.* **2021**, *6*, 3567–3571.
- [56] G. Tsotridis, A. Pilenga, *European Commission: Brussels, Belgium* **2021**.
- [57] Y. Uchino, T. Kobayashi, S. Hasegawa, I. Nagashima, Y. Sunada, A. Manabe, Y. Nishiki, S. Mitsushima, *Electrocatalysis* **2017**, *9*, 67–74.
- [58] Y. Kim, S. M. Jung, K. S. Kim, H. Y. Kim, J. Kwon, J. Lee, H. S. Cho, Y. T. Kim, *JACS Au* **2022**, *2*, 2491–2500.
- [59] A. Abdel Haleem, K. Nagasawa, Y. Kuroda, Y. Nishiki, A. Zaenal, S. Mitsushima, *Electrochemistry* **2021**, *89*, 186–191.

Manuscript received: August 25, 2023

Revised manuscript received: October 31, 2023

Version of record online: December 4, 2023